Study of meteor characteristics over Gadanki using VHF radar observations

A. Guharay[1,*], K. Chenna Reddy[2], D. Chakrabarty[3] and G. Yellaiah[2]

[1]National Institute for Space Research, Sao Jose dos Campos, 12227-010, Sao Paulo, Brazil
[2]Department of Astronomy, Osmania University, Hyderabad 530 003, India
[3]Physical Research Laboratory, Navrangpura, Ahmedabad 380 009, India

Meteor characteristics during shower and non-shower periods in 2005–2008 have been studied using narrow beam (HPBW ~3°) VHF radar at Gadanki (13.5°N, 79.2°E). Various interesting echoes are illustrated and probable explanations for their behaviour are also provided. Doppler spectra of the Range Spread Trail Echo indicate a probable plasma convergence and gradient drift instability associated plasma turbulence in some cases.

Keywords. Field-aligned irregularities, meteor echoes, plasma instability, radar observations.

EVERY day tonnes of materials (total mass flux ~10^7 kg/year) of extraterrestrial origin hit the Earth's atmosphere from various directions, which are called meteoroids[1]. Due to collision of high-velocity (~11–72 km/s) meteoroids with the air molecules the temperature can reach up to 2500 K (depending on composition, size and speed) which is followed by ionization of the surface molecules of the meteoroid and the surrounding air. This ionization which is formed in a cylindrical shape and centred about the meteoroid trajectory is known as trail. Echoes in the radio signal are obtained from the ionization formed surrounding the meteoroid body (during the passage of the meteoroid) and trail (after the passage of the meteoroid) mostly within the altitude range ~70–140 km. The radar-detected meteors are mostly called micrometeoroids, since they comprise of materials in the size of microns. The minimum size of the meteoroid which can produce meteor phenomenon is roughly 10 μm (ref. 1).

There are mainly two kinds of major echoes classified on the basis of geometry of the meteoroid path and the detecting radar beam direction. If the direction of the meteor trail is perpendicular to the beam direction for single station observation, then the return is called specular echo. On the other hand, if the meteor trail is almost parallel to the beam it is called non-specular or down-the-beam echo. Head echo is a special type of non-specular echo existing over a number of range bins of the radar for a very short time due to the scattering of radio waves from the plasma surrounding the ablating meteoroid[2]. Comparatively long-lasting echoes coming from the series of trails over continuous range bins soon after the head echo are called range spread trail echos (RSTEs)[3] or spread meteor echos (SMEs)[4]. Interesting properties of the non-specular trail echoes were studied several researchers in the last couple of decades[5–7]. In addition, various other kinds of echoes are also classified by Valentic *et al.*[8] using narrow-band VHF radar observations over Adelaide (35°S, 138°E). At the initial stage of trail formation, the density of the electrons remains very high (> 10^{15}/m). The return from such plasma is called over-dense echo. With the passage of time, the plasma density diminishes due to ambipolar diffusion in association with radial expansion of the ionization cylinder. Echo produced at this stage is called under-dense echo (electron density ~< 10^{13}/m). Production of excessive heat due to high kinetic energy of the meteoroid can generate large pressure on it and cause fragmentation of the main body into several pieces. Various aspects of the fragmentation process were studied extensively by several investigators[3,9].

Meteor trail-related plasma irregularities were first observed by Heritage *et al.*[10] using VHF radar observations. Chapin and Kudeki[5] inferred that the equatorial E region long-duration non-specular echo is predominately caused by gradient-drift Farley–Buneman (GDFB) instability, which rapidly develops into plasma turbulence. Using simulation of meteor trail in the equatorial electrojet region, Oppenheim *et al.*[11] showed that the occurrence of the GDFB instability is related to high electric field and trail density gradient. Such high electric field in association with high-density gradient near the edge of the trail excites the plasma wave. Such a wave generates an anomalous cross-field ($\perp\mathbf{B}$) diffusion, which can be greater than the cross-field ambipolar diffusion by an order of magnitude[12]. Reddi and Nair[13] studied Doppler spectra of SME created by short-lived meteor trail using MST radar over the present observation site. They found asymmetric distribution of peaks in Doppler spectra with very high Doppler velocities. Although various meteor characteristics have been studied by past investigators, our knowledge of the underlying physical mechanisms behind the observed features is limited. In the present work, we have studied some basic meteor characteristics over Gadanki (13.5°N, 79.2°E, magnetic dip lat. ~6.3°N) with observations during Perseid, Geminid showers and also some non-shower periods in 2005–2008 with the help of narrow-beam VHF radar observations.

We have used the VHF radar at the National Atmospheric Research Laboratory, Gadanki. It operates with a frequency of 53 MHz with peak power aperture product of 3×10^{10} Wm^2. It utilizes 32×32 Yagi antenna distributed in a square-phased array. Detailed specifications of the radar can be found in the existing literature[14]. Pulse

*For correspondence. (e-mail : guharay@laser.inpe.br)

Table 1. Observational statistics of meteor echoes

Year	Start time		End time		Duration (h)	Total no. of echoes
	Date	Time (LT)	Date	Time (LT)		
2005	12 December†	20 : 27 : 30	13 December	07 : 00 : 58	~ 10 : 27	83
	13 December†	19 : 00 : 42	14 December	05 : 55 : 18	~ 10 : 55	87
	14 December†	19 : 03 : 41	15 December	06 : 23 : 36	~ 11 : 20	102
2006	5 August	21 : 56 : 57	6 August	05 : 50 : 11	~ 07 : 53	99
	6 August	06 : 45 : 55	6 August	12 : 00 : 15	~ 05 : 15	117
	6 August	14 : 01 : 50	6 August	17 : 20 : 07	~ 03 : 18	30
	6 August	19 : 19 : 10	6 August	22 : 06 : 57	~ 02 : 40	11
	11 August*	22 : 04 : 03	12 August	00 : 15 : 51	~ 02 : 11	13
	12 August*	01 : 13 : 17	12 August	06 : 17 : 05	~ 05 : 04	71
	12 August*	21 : 57 : 32	13 August	05 : 56 : 34	~ 08 : 00	70
	13 August*	07 : 01 : 26	13 August	11 : 59 : 48	~ 05 : 01	52
	13 August*	14 : 00 : 05	13 August	17 : 20 : 49	~ 03 : 20	46
	13 August*	19 : 11 : 01	12 August	06 : 00 : 18	~ 09 : 49	96
2007	1 December*	20 : 01 : 20	2 December	00 : 01 : 40	~ 04 : 20	20
	11 December†	19 : 59 : 21	12 December	05 : 57 : 06	~ 10 : 00	106
	12 December†	19 : 54 : 02	13 December	05 : 31 : 00	~ 09 : 37	56
	13 December†	20 : 02 : 42	14 December	06 : 02 : 44	~ 18 : 00	74
	14 December†	19 : 50 : 13	15 December	06 : 06 : 01	~ 10 : 15	90
2008	26 June	11 : 02 : 01	26 June	23 : 45 : 17	~ 12 : 43	78
	27 June	00 : 18 : 30	27 June	09 : 20 : 30	~ 09 : 02	107
	10 August*	00 : 25 : 20	10 August	06 : 31 : 24	~ 06 : 06	38
	11 August*	18 : 39 : 56	12 August	05 : 58 : 13	~ 11 : 18	48
	12 August*	09 : 30 : 08	12 August	18 : 15 : 46	~ 08 : 45	32
	12 August*	18 : 43 : 59	13 August	08 : 58 : 23	~ 14 : 15	80
	13 August*	18 : 02 : 56	14 August	06 : 32 : 04	~ 12 : 30	42

Events marked with † and ∗ represent Geminid and Perseid showers respectively. Unmarked events represent non-shower period.

repetition frequency (PRF) and pulse width (PW) can be selected in binary multiples. It has six steerable beam directions with beam width of ~ 3°. The directions are one towards zenith, four towards magnetic N, S, E, W at zenith angle 20° and one beam of zenith angle 13.6° towards magnetic north. Signal from the echoes is recorded in inphase (*I*) and quadrature (*Q*) components with maximum 1024 samples in each data block. *I* and *Q* data are recorded continuously during the observational period and meteor echoes are identified manually.

For the present study we have chosen PRF of 1000 and PW of 8 μs. This PW value gives range resolution of 1.2 km within the observed range 80–120 km of total 34 bins. Signal from four consecutive transmitter pulses is averaged to obtain the time interval between successive samples of 4 ms. Thus each data block consisting of *I* and *Q* components records the backscattered signal for 4.096 s. Hence the complex Doppler spectrum calculated from the *I* and *Q* components for each range bin contains Nyquist frequency of 125 Hz or maximum attainable Doppler velocity of 353.8 m/s. The radar was operated in campaign mode during shower and non-shower periods. Details of the observation statistics are provided in Table 1.

Diurnal variation of the occurrence rate (over an hourly interval) of the detected meteor echoes over during 12–13 August 2008 when consistent data reception over time and range is available is shown in Figure 1 *a*. Occurrence rate decreases monotonically after starting from 1000 LT until 1400 LT (12 August 2008). Thereafter, it shows almost constant value with successive rise and fall up to 2300 LT. From 00 LT (13 August 2008), the occurrence rate increases rapidly and reaches a maximum at 0500 LT. The average hourly occurrence rate after this time remains quite high compared to the rest of the diurnal cycle. Figure 1 *b* shows the occurrence rate (over a kilometre height interval). It exhibits quite a large value near 98–100 km, with a maximum at 98 km. The height of maximum occurrence rate is higher in comparison with a few earlier studies from mid and low latitudes by Nakamura *et al.*[15] (~ 88 km), Selvamurugan *et al.*[16] (90 km) and Kumar *et al.*[17] (~ 92 km). Occurrence rate also reveals a secondary peak near 106–108 km. According to a few earlier studies, maximum kinetic energy deposition and deceleration of the meteoroid mainly take place near 105 km altitude[1,2], which could be the reason for the secondary maximum.

Power (in arbitrary units) variation of some interesting backscattered echoes due to Fresnel diffraction is shown in Figure 2. Figure 2 *a* shows an over-dense echo due to passage of a meteoroid almost perpendicular to the radar

beam and hence almost symmetric rise and decay of the backscattered signal is observed, which represents Gaussian-shaped main lobe of the antenna. Small-scale fluctuations are embedded on the main varying envelope, probably due to non-uniform ionization along the trail which creates several scattering points over it. Figure 2 *b* shows another example of an over-dense echo where the signal is much smoother compared to the previous example. Here the power shows three evident broad maxima unlike the previous one. Such a phenomenon takes place probably due to the presence of multiple meteor trails within the radar beam with finite time gap among them. This kind of situation may arise when trails (can be caused by fragmentation) drift into the radar field-of-view after creation by background wind. Figure 2 *c* exhibits well-spaced oscillations with inappreciable small-scale fluctuations. Such a phenomenon (alternative crests and troughs) can be interpreted as interference of backscattered signals from two trails with uniform ionization within the beam exposure time. The formation of these closely spaced trails is most probably due to fragmentation. Figure 2 *d* shows one interesting pattern of variation where well-shaped large scale crests contain small-scale regular fluctuations. This is also a probable outcome of fragmentation effect. Small-scale fluctuations can be attributed to the multiple scattering points of the individual trail. Figure 2 *e* shows a typical example of classical under-dense echo where the echo strength rises fast and decays exponentially due to diffusion. Small-scale irregularities are also visible in the echo signal. Finer details of such kind of echo phenomena can only be acquired by a more extensive study, which is beyond the scope of the present study.

Figure 3 *a* shows range time intensity (RTI) and Figure 3 *b* amplitude variation plots of a typical head echo and long-duration RSTE conspicuous over 13 range bins. The straight line in Figure 3 *b* at the leading edge of the fluctuations indicates the head echo. Unfortunately, only data over 1 s span are available for this frame. Head echo is prominent over a large number of range bins and trail echoes are observed to form at comparatively lower altitude. Also at the lowest altitude the backscattered signal shows broad peaks with less amplitude of fluctuation. Geocentric velocities estimated from the head echo slope during various shower periods come out to be ~ 46 ± 6 km/s in August 2006 (Perseid), 50 ± 5 km/s in December 2007 (Geminid), 44 ± 7 km/s in June 2008 and 42 ± 6 km/s in August 2008 (Perseid).

Doppler spectra of RSTE echoes detected at successive range bins of the beam directed at 13°N, Z, 20°E and

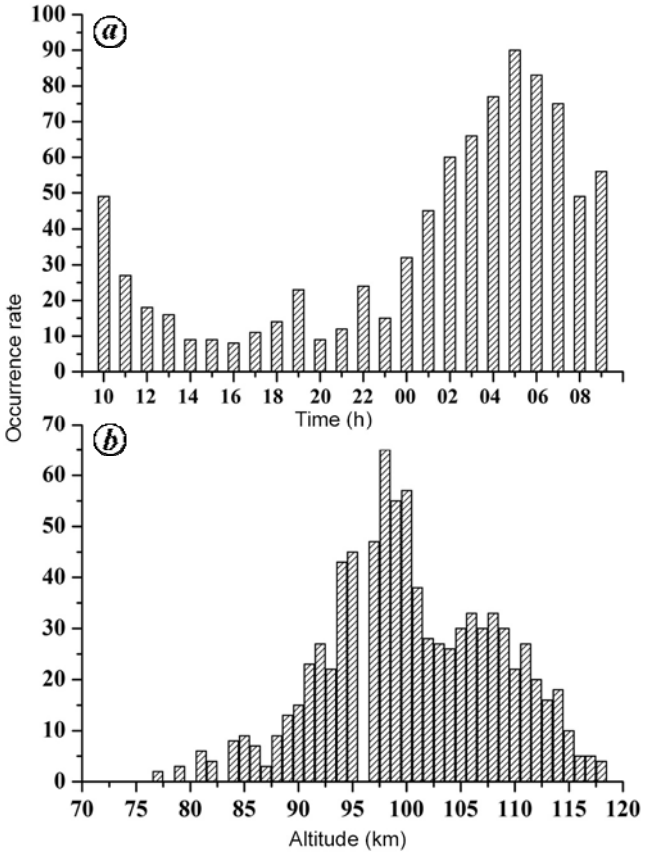

Figure 1. Diurnal variation of meteor occurrence rates shown with (***a***) time and (***b***) altitude on 12–13 August 2008.

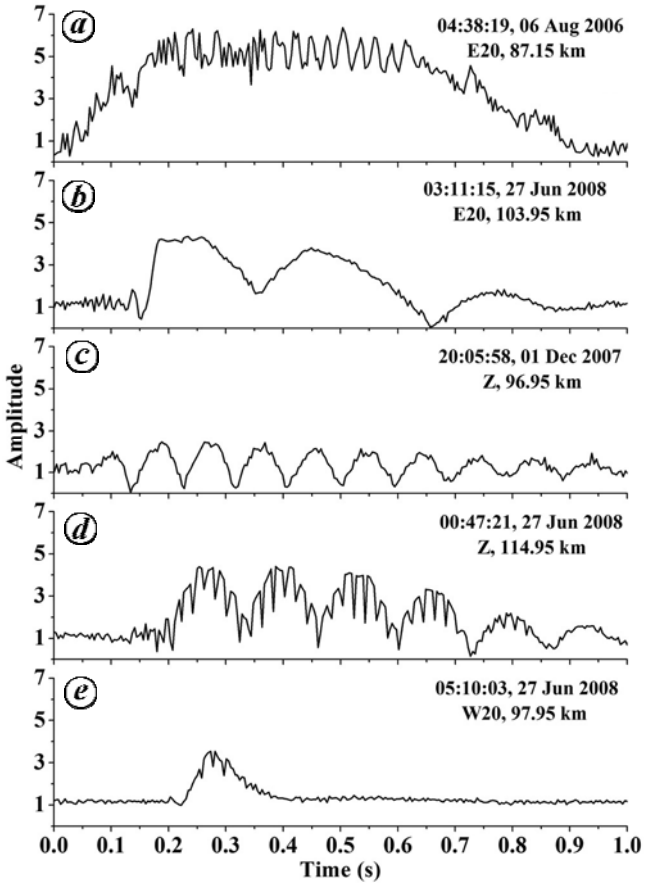

Figure 2. Some interesting echoes observed during 2005–2008 for various beam directions. For details see text.

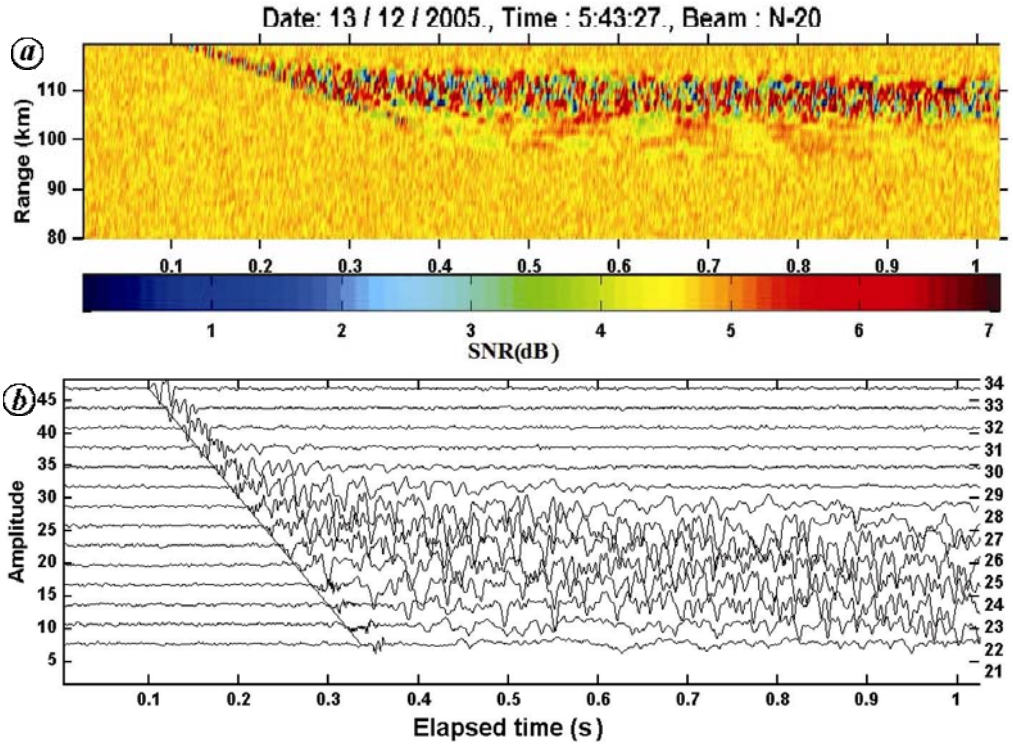

Figure 3. (***a***) Range time intensity (RTI) and (***b***) amplitude (arbitrary units) plot of a typical meteor echo clearly showing head (straight line) and trail (continuing fluctuations) echoes.

20°W are estimated with respect to line of sight Doppler velocity (Figure 4). The top and bottom bins of each spectrum represent the noise spectrum. Most of the range bins exhibit negative Doppler velocity. Spectra of most of the beams reveal several non-Gaussian sharp peaks in each range bin, except the west beam which contains relatively broader and smoother peaks generally at higher range (altitude). All the spectra exhibit maximum magnitude of the dominant Doppler velocity peak in each range bin within 180 m/s. North and zenith beams show negative velocity peaks. East beam reveals negative velocity at higher altitude, which turns gradually to positive values in the lower altitude region. In the west beam peaks are distributed on the negative side of the velocity and a few maxima are also observed at the positive side at lower altitude.

The present results point out several interesting features of the meteor echoes over the Indian low-latitude station, which are discussed here in the light of the existing literature. According to Close *et al.*[2], maximum number of echoes near 105 km can be attributed to the higher radar cross-section (RCS) at this altitude. At higher altitude (> 105 km) due to higher mean free path, the plasma diffuses faster which causes diminution of the RCS even for high ionization rate. At lower altitude (< 105 km) as the mean free path is lower (less diffusion), the radius of the plasma scattering zone becomes smaller which in turn reduces the RCS. In this context it is interesting to mention that using rocket observations over an Indian low-latitude station which is close to the present observation site during the Leonid shower, Gupta *et al.*[18] found maximum amplitude of plasma wave of sub-metre size near 105 km.

Aspect sensitivity of the backscattered echoes from the meteor is one of the most important features studied so far. To the best of our knowledge, Heritage *et al.*[10] first reported the alignment of the meteor trail-generated irregularities along magnetic field lines with VHF radar observations. Reddi and Nair[13] explained that the RSTEs were formed due to the formation of striations parallel to the magnetic field with VHF radar observations from the present site. Later, Reddi *et al.*[4] observed RSTE from the trails aligned parallel to the radar beam and not parallel to the magnetic field, which seems to be quite different compared to the results mentioned earlier. Using MU radar observations, Zhou *et al.*[19] inferred that the field-aligned irregularities (FAI) are responsible for generation of RSTEs. They observed that most of the detected RSTEs were due to the geometry of the radar beam direction perpendicular to the magnetic field and there was practically no echo for radar beam direction parallel to the magnetic field. Strength of the RSTE is generally much weaker than the classical specular echo. Classical specular echo is produced due to coherent scattering of the electrons mostly from one Fresnel zone. On the other hand, RSTE is produced due to density fluctuation of the

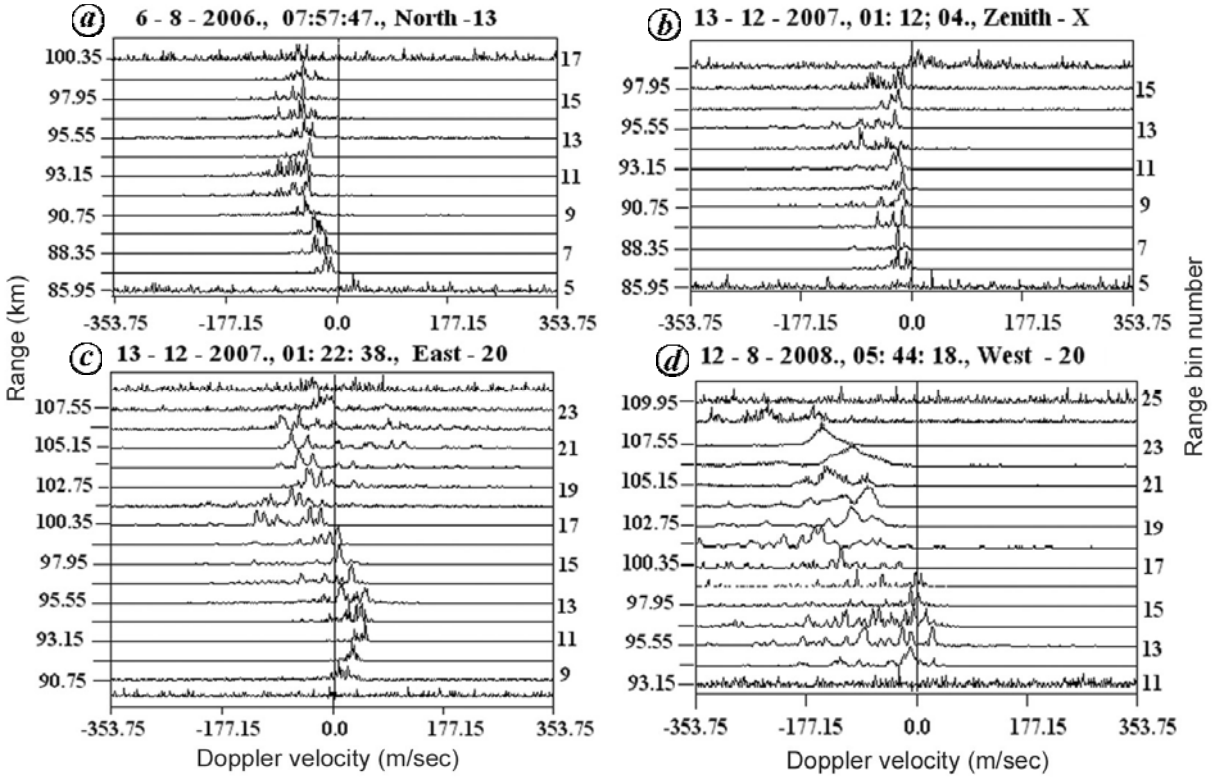

Figure 4. Doppler velocity spectra of good echoes obtained at four beam directions over various range bins.

FAI[19]. Malhotra *et al.*[7] found longer duration meteor echoes when the radar beam was perpendicular to the geomagnetic field in comparison with other directions. They also mentioned that at the initial stage of trail formation, the echo can be obtained from any direction. The trail tries to align along the magnetic field with time until it gets completely aligned along the magnetic field. Hence at this stage the echo can only be observed if the radar beam directs nearly perpendicular to the magnetic field. In the present case we have observed non-specular echoes at all possible directions corresponding to the selected beam angles. It should also be mentioned that our observation is limited to maximum 4 s continuous data record duration. Hence such a phenomenon indicates the record of data for the initial phase of the long-duration echoes for the present case. Therefore, long-duration exposure can give actual insight of the various phases of the meteor trail evolution which can be pursued in future.

Spectra of the N13 and Z beams reveal negative Doppler velocity which is possibly due to the vertical $\mathbf{E} \times \mathbf{B}$ drift of ionization caused by the eastward electric field. N13 spectrum also indicates a crossover of the eastward electric field to the westward direction at lowest altitude, implying a shear zone. In this context it should be mentioned that strong wind shear can generate plasma irregularities due to density fluctuations, which is able to cause RSTE[6]. It is interesting to note that the E20 spectrum shows negative velocity (westward electric field) at higher altitude, which changes to positive velocity (eastward electric field) at lower altitude. Such orientation of the electric field causes downward motion of the ionization at higher altitude and upward motion of the same at lower altitude due to $\mathbf{E} \times \mathbf{B}$ drift, which results in the formation of a convergence zone. Denardini *et al.*[20] found the important role of the gravity waves significantly in altering the vertical gradient of the *E*-region electric field with observations from a Brazilian dip equatorial station, Sao Luis (2.3°S, 44.2°W, dip: –0.5°). Gravity waves are also supposed to be crucial in causing reversal of the electric field by creating strong wind shear[21], which could be a probable reason for the creation of the convergence zone as observed in the present study. Narrow spectral peaks for the most of the beams may indicate the presence of type-1 instability, but sufficiently low velocity (< 180 m/s) precludes such possibility. Comparatively broad maxima in W20 spectra at higher altitude indicate a possible role of type-2 instability. The most likely mechanism responsible for such occurrence is gradient drift instability. We have also found finite time delay of 25–40 ms between head and trail echoes for these spectra, which indicates the possible role of GDFB instability[2,22]. Dyrud *et al.*[22] explained this time delay as necessary for plasma instability to grow enough to be visible in the radar. Using model simulation, Oppenheim *et al.*[11] mentioned the generation of an ambipolar electric field normal to both magnetic field and trail length. Subsequently,

the $\mathbf{E} \times \mathbf{B}$ drift of the electrons over the axis of the meteor trail plays an important role to drive the GDFB instability and associated plasma density waves followed by plasma turbulence. Plasma turbulence breaks the trail into various segments and forms the FAI, which causes non-specular trail echoes in the radar. Chu and Wang[6] mentioned that the field-aligned plasma irregularities in the RSTE are caused by wind shear, which is found to be different compared to the GDFB instability mechanism discussed earlier. Reddi and Nair[13] argued that finite delay (20–200 ms) between head and spread echoes cannot be considered as a sole effect of cross-field or gradient drift instability. Large density gradient (10^3–10^4/m^3/m) of electrons perpendicular to the trail should initiate diffusion before any other instability takes place.

Sharp spectral peaks with deep minima are possibly due to discrete scattering centres[13]. Observed asymmetric nature of the dominant high frequencies in all the spectra agrees with the initial Doppler spectra of the long-duration meteor echoes studied by Chapin and Kudeki[5] using Jicamarca VHF radar. They reported that the initial asymmetric spectral peaks became nearly symmetric with time. Such asymmetric behaviour of the Doppler spectra was also reported by other investigators[4,13,19]. Recently, Chu and Wang[6] noted asymmetric peaks over a large range of altitude with smaller Doppler velocities using Chung-Li VHF radar observations for short-duration echoes.

1. Ceplecha, Z., Borovicka, J., Elford, W. G., ReVelle, D. O., Hawkes, R. L., Porubcan, V. and Simek, M., Meteor phenomena and bodies. *Space Sci. Rev.*, 1998, **84**, 327–471; doi: 10.1023/A:1005069928850.
2. Close, S., Oppenheim, M., Hunt, S. and Dyrud, L., Scattering characteristics of high-resolution meteor head echoes detected at multiple frequencies. *J. Geophys. Res. A*, 2002, **107**; doi: 10.1029/2002JA009253.
3. Mathews, J. D., Briczinski, S. J., Malhotra, A. and Cross, J., Extensive meteoroid fragmentation in V/UHF radar meteor observations at Arecibo Observatory. *Geophys. Res. Lett.*, 2010, **37**, L04103; doi: 10.1029/2009GL041967.
4. Reddi, C. R., Sarma, T. V. C. and Rao, P. B., Spatial domain interferometric VHF radar observations of spread meteor echoes. *J. Atmos. Sol.–Terr. Phys.*, 2002, **64**, 339–347; doi: 10.1016/S1364-6826(01)00107-9.
5. Chapin, E. and Kudeki, E., Radar interferometric imaging studies of long-duration meteor echoes observed at Jicamarca. *J. Geophys. Res.*, 1994, **99**, 8937–8949.
6. Chu, Y.-H. and Wang, C.-Y., Interferometry observations of VHF backscatter from plasma irregularities induced by meteor in sporadic E region. *Geophys. Res. Lett.*, 2003, **30**; doi: 10.1029/2003GL017703.
7. Malhotra, A., Mathews, J. D. and Urbina, J., A radio science perspective on long-duration meteor trails. *J. Geophys. Res.*, 2007, **112**, A12303; doi: 10.1029/2007JA012576.
8. Valentic, J. A., Avery, J. P., Avery, S. K., Cervera, M. A., Elford, W. G., Vincent, R. A. and Reid, I. M., A comparison of meteor radar systems at Buckland Park. *Radio Sci.*, 1996, **31**, 1313–1329.
9. Kero, J., Szasz, C., Pellinen-Wannberg, A., Wannberg, G., Westman, A. and Meisel, D. D., Three-dimensional radar observation of a submillimeter meteoroid fragmentation. *Geophys. Res. Lett.*, 2008, **35**, L04101; doi: 10.1029/2007GL032733.
10. Heritage, J. L., Fay, W. J. and Bowen, E. D., Evidence that meteor trails produce a field-aligned scatter signal at VHF. *J. Geophys. Res.*, 1962, **67**, 953–959.
11. Oppenheim, M. M., Endt, A. F. and vom Dyrud, L. P., Electrodynamics of meteor trail evolution in the equatorial E-region ionosphere. *Geophys. Res. Lett.*, 2000, **27**, 3173.
12. Dyrud, L. P., Oppenheim, M. M. and vom Endt, A. F., The anomalous diffusion of meteor trails. *Geophys. Res. Lett.*, 2001, **28**, 2775–2778; doi: 10.1029/2000GL012749.
13. Reddi, C. R. and Nair, S. M., Meteor trail induced backscatter in MST radar echoes. *Geophys. Res. Lett.*, 1998, **25**, 473–476.
14. Rao, P. B., Jain, A. R., Kishore, P., Balamuralidhar, P., Damle, S. H. and Viswanathan, G., Indian MST radar. 1. System description and sample vector wind measurements in ST mode. *Radio Sci.*, 1995, **30**, 1125–1138.
15. Nakamura, T., Tsuda, T., Tsutsumi, M., Kita, K., Uehara, T., Kato, S. and Fukao, S., Meteor wind observations with the MU radar. *Radio Sci.*, 1991, **26**, 857–869; doi: 10.1029/91RS01164.
16. Selvamurugan, R., Devasia, C. V., Jain, A. R., Raghava Reddi, C., Rao, P. B. and Sridharan, R., Observations on stratospheric–mesospheric–thermospheric temperatures using Indian MST radar and co-located LIDAR during Leonid Meteor Shower (LMS). *Ann. Geophys.*, 2002, **20**, 1869–1876; doi: 10.5194/angeo-20-1869-2002.
17. Kumar, K. K., Rankumar, G. and Shelbi, S. T., Initial results from SKiYMET meteor radar at Thumba (8.5°N, 77°E): 1. Comparison of wind measurements with MF spaced antenna radar system. *Radio Sci.*, 2007, **42**, RS6008; doi: 10.1029/2006RS003551.
18. Gupta, S. P., Sekar, R. and Acharya, Y. B., *In situ* measurements of sub-meter plasma waves over low-latitude ionosphere during Leonid-99 meteor storm. *Ann. Geophys.*, 2004, **22**, 2033–2036; doi: 10.5194/angeo-22-2033-2004.
19. Zhou, Q. H., Mathews, J. D. and Nakamura, T., Implications of meteor observations by the MU radar. *Geophys. Res. Lett.*, 2001, **28**, 1399–1402.
20. Denardini, C. M., *et al.*, E region electric fields at the dip equator and anomalous conductivity effects. *Adv. Space Res.*, 2012; http://dx.doi.org/10.1016/j.asr.2012.06.003.
21. Denardini, C. M. *et al.*, Counter electrojet features in the Brazilian sector: simultaneous observation by radar, digital sounder and magnetometers. *Ann. Geophys.*, 2009, **27**, 1593–1603.
22. Dyrud, L. P., Oppenheim, M. M., Close, S. and Hunt, S., Interpretation of non-specular radar meteor trails. *Geophys. Res. Lett.*, 2002, **29**, doi: 10.1029/2002GL015953.

ACKNOWLEDGEMENTS. We thank the Director, National Atmospheric Research Laboratory for providing the necessary data. The work is partially supported by the Department of Space, Government of India. A.G. thanks FAPESP, Sao Paulo, Brazil for financial support.

Received 24 September 2012; accepted 8 April 2013